Sensor Integration of 3D Map Aided GNSS and Smartphone PDR in Urban Canyon with Dense Foliage

Li-Ta Hsu, Yanlei Gu and Shunsuke Kamijo
Institute of Industrial Science
The University of Tokyo
4-6-1 Komaba, Meguro-ku, Tokyo, Japan
qmohsu@kmj.iis.u-tokyo.ac.jp, guyanlei@kmj.iis.u-tokyo.ac.jp and kamijo@iis.u-tokyo.ac.jp

***Abstract*— Pedestrian localization service is required in deep urban canyons. Many studies demonstrated the potentials of 3D building model to GNSS positioning, especially in city center areas. However, many narrow building canyon also contains dense foliage of street trees. This foliage not only strongly attenuates but also blocks the line-of-sight (LOS) visible GNSS signals. The number of the trackable satellites is hence greatly decreased to less than 4, which GPS receiver cannot provide positioning result. Even through the commercial GNSS receiver implemented strong filtering technique to provide the positioning solutions during the signal blockage, the results are usually erroneous. This research proposes to integrate a 3D map aided GNSS (3D-GNSS) with a smartphone-based pedestrian dead reckoning (PDR) to provide localization service in urban area with dense foliage.**

Keywords—Global Positioning System, Multipath, Pedestrian, Dead Reckoning, 3D maps, Foliage, Urban Canyon, Smartphone

I. INTRODUCTION

Navigation service for vision-impaired pedestrian receives a lot of attention recently. Pedestrians are walking in all kinds of environments, including open fiend, sub-urban streets, deep urban streets and indoor environments. Global navigation satellite system (GNSS) receivers can achieve highly accurate positioning performance in the first two areas. Due to the degrading of signal transmission, GNSS signal could almost not able to be received in indoor areas [1]. In the deep urban canyon, a few number of GNSS signals can be received, but its accuracy is greatly affected by the notorious multipath effects and non-line-of-sight (NLOS) reception [2]. Researchers have been intensively studying the possibilities to improve GNSS navigation performance in urban canyons [3-5]. Since 2007, using 3D building models (or so-called 3D maps and city models) as aids to mitigate/exclude/correct the multipath and NLOS effects has become a popular approach to enhance GNSS receivers [6-9]. The detail introduction of the related work of the 3D map aided GNSS can be found in [10]. Our group previously proposes an innovative GPS error correction method by the use of 3D building model and ray-tracing simulation [11]. We called it 3D-GNSS. The benefit of using QZSS signals and L1-SAIF corrections for 3D-GNSS is previously evaluated [12]. We also adopted it with multi-GNSS measurements and proposed the reliability calculation for this 3D-GNSS [13]. In addition, the exclusions of the double or multiple reflected NLOS using receiver autonomous integrity monitoring (RAIM) fault detection and exclusion (FDE) for this 3D-GNSS is also proposed [14]. However, the 3D-GNSS still suffers from the low availability in the area of deep urban canyon with dense foliage because of the lack of received satellites. Unlike the buildings, the dense foliage of street trees even block the satellites in even more than 80^{o} of elevation angle. Other alternative sensors are required to continue the navigation service for the vision impaired pedestrian. We have developed a smartphone-based PDR previously [15]. The developed smartphone PDR is put in the pocket of pedestrian. Finally, we integrate the 3D-GNSS with the smartphone-based PDR using an adaptive loosely-coupled Kalman filter developed in this paper. Accordingly, this paper is organized as follow: The problem statement is given in Section II. Kalman filter integration is introduced in Section III. Experimental results are shown in Section IV. Finally, the concluding remarks are given in Section V.

II. PROBLEM STATEMENT

In Tokyo city center, there are many deep urban canyons such as Shinjuku, Marunouchi, Shibuya and Ginza areas. In these areas, not only density of building but also the height of building are high. In addition, the dense foliage of the street trees is devastating to GNSS receiver especially for pedestrian navigation. The foliage is changing by the seasons. Right and left of Fig. 1 demonstrate an urban canyon with dense street trees in winter and summer seasons, respectively.

Fig. 1. Foliage of street trees in winter and summer seasons.

978-1-5090-2042-3/16/$31.00 © 2016 IEEE

It is obvious that the densities of the foliage are different, hence, the performances of GNSS receiver are also different. We conducted pedestrian tests in both the winter and summer times. The test environments are shown in Figs. 1 and 2. We walked in straight line in the pedestrian walk as shown in Fig. 2(b). The number of satellite received in the experiments in winter and summer are shown in Figs. 3 and 4.

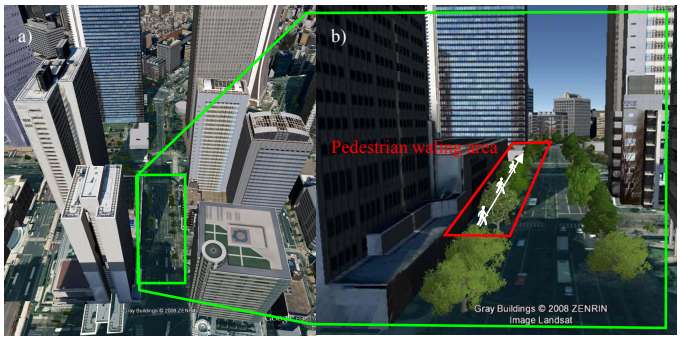

Fig. 2. Demonstration of the target deep urban canyon with dense foliage.

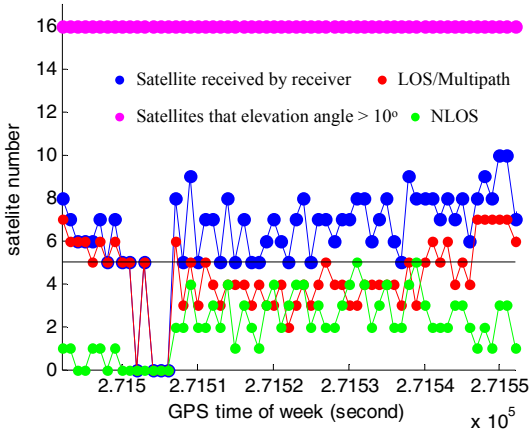

Fig. 3. Number of Satellites in the dense urban canyon without dense foliage.

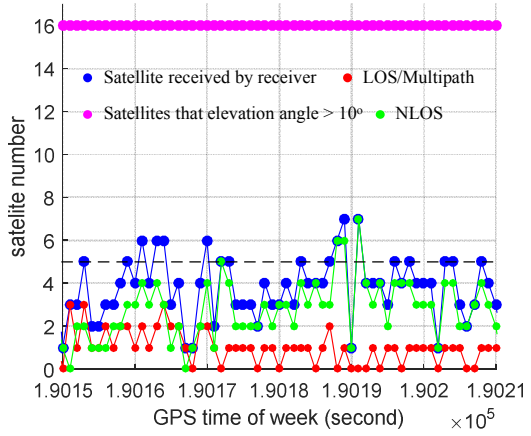

Fig. 4. Number of Satellites in the dense urban canyon with dense foliage.

The pink dot indicates the number of satellite that its elevation angle is higher than 10^{o} (not necessary to be received by receiver due to signal blockages). The blue dot indicates the number of satellites received by a commercial GNSS receiver, u-blox M8N is used. The red and green dot indicate the type of the received satellite is LOS visible or NLOS, respectively. The classification is done using both 3D maps and ray-tracing simulation from the ground truth location [13]. Comparing Figs. 3 and 4, firstly, the pink dots are the same which means the satellite conditions are similar. Secondly, the number of LOS visible (red dot) satellite in Fig. 3 is more than that in Fig. 4. This decrease implies that the dense foliage blocks most of the LOS satellite in deep urban canyon. It is interesting to note that the numbers of NLOS (green dot) are similar in Figs 3 and 4. This is because the reflections are not fully blocked by foliage as shown in Fig 5.

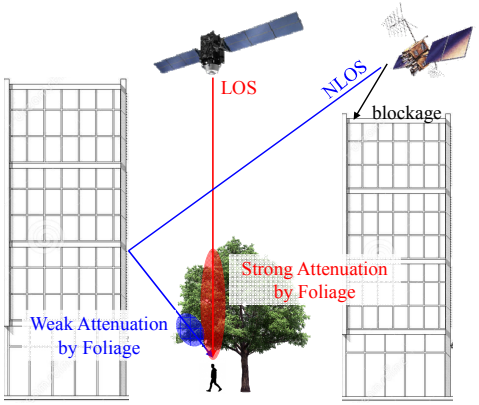

Fig. 5. Illustration of the foliage attenuation to LOS and NLOS signals.

Comparing to LOS signal, NLOS signal travels through less leafs. As a result, NLOS signal is still trackable in the dense foliage environments. In the contrary, LOS signal is usually blocked. Although 3D-GNSS could correct the single reflected NLOS delay, the number of received satellites is usually less than 5, which makes 3D-GNSS impossible to always give solutions. In this case, inertial sensor is a good candidate to continue the navigation service. In this paper, we implement a pocket-based smartphone PDR to provide the dynamic model of pedestrian. The detail algorithm of this smartphone PDR can be found at [15]. We therefore use a Kalman filter to integrate 3D-GNSS with the PDR, which introduced in the next section.

III. CLOSED-LOOP KALMAN FILTER

The flowchart of the integration system is shown in Fig .6.

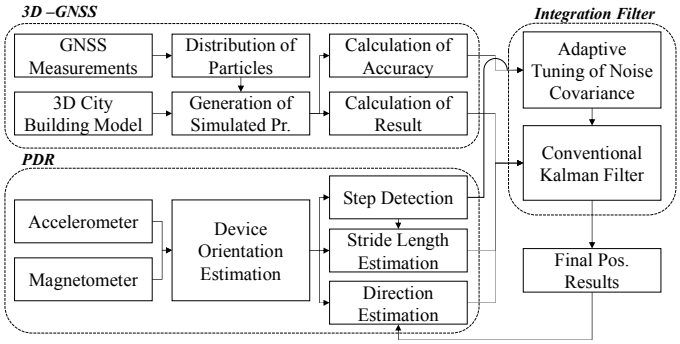

Fig. 6. Flowchart of the integration system.

3D-GNSS [11] and smartphone PDR [15] results are used as measurement and system input, respectively.

A. Setup of Kalman Filtering

We implement a total state closed loop Kalman filter. The observed states are:

$$\boldsymbol{X_i} = [x_i \quad y_i \quad \theta_i]^{\boldsymbol{T}} \tag{1}$$

where x_i, y_i, and θ_i denote the longitude, latitude and heading angle, respectively. 3D-GNSS provides the position and heading angle as measurements to the Kalman filter as shown below:

$$\boldsymbol{z} = [x_i^{3D-GNSS} \quad y_i^{3D-GNSS} \quad \Theta_i^{3D-GNSS}]^T \tag{2}$$

Thus, the observation matrix, $\boldsymbol{H}$, is an identity. The smartphone-based PDR provides the system input for the Kalman filter as shown in (3).

$$\mathbf{u_i} = \begin{bmatrix} d \cdot cos(\theta_i^{PDR} - \delta\theta) \\ d \cdot sin(\theta_i^{PDR} - \delta\theta) \\ \theta_i^{PDR} - \delta\theta_i \end{bmatrix} \tag{3}$$

where d denotes the walking distance per second obtained by the PDR. $\delta\theta_i$ denotes the heading angle correction. It is calculated by the difference between the previous raw heading angle estimated by PDR and the previous updated heading angle by the Kalman filter as shown in (4).

$$\delta\theta_i = \theta_{i-1}^{PDR} - \theta_{i-1}^{+} \tag{4}$$

where the superscript "+" denotes the updated state of the Kalman filter. By the use of the heading angle correction, the heading offset of PDR can be mitigated. We use a simple propagation model as:

$$\boldsymbol{F} = \begin{bmatrix} 1 & 0 & 0 \\ 0 & 1 & 0 \\ 0 & 0 & 0 \end{bmatrix} \tag{5}$$

As can be seen from (5), the position remains the previous position if no step detected in the PDR system.

B. Adaptive Tuning of Noise Covariance

There are two factors to affect the reliability of 3D-GNSS positioning method, distribution of particles and pseudorange similarity of particles. The noise variance of the positioning performance of the 3D-GNSS can be calculated as (6).

$$\sigma^{3D-GNSS^2} = \left(\overline{d_{pr}^{(j)}}\right)^2 \times HDOP^{3D-GNSS}, \tag{6}$$

where $HDOP^{3D-GNSS}$ denotes the horizontal dilution of precision (HDOP) of particles in the 3D-GNSS. The detail calculation of the $HDOP^{3D-GNSS}$ can be found in [13]. To calculate the possible maximum heading angle estimated by the 3D-GNSS, the previous calculated $\sigma_{3D-GNSS}^2$ is used.

$$\boldsymbol{R_i} = \begin{bmatrix} K\sigma_i^{3D-GNSS^2} & 0 & 0 \\ 0 & K\sigma_i^{3D-GNSS^2} & 0 \\ 0 & 0 & \Theta_i^{3D-GNSS^2} \end{bmatrix} \tag{7}$$

where K denotes a constant factor, which is empirical set as 4 in this paper. The propagation noise covariance matrix used is shown in (8).

$$\boldsymbol{Q} = \begin{bmatrix} K^{PDR} & 0 & 0 \\ 0 & K^{PDR} & 0 \\ 0 & 0 & K^{\vartheta} \end{bmatrix} \tag{8}$$

The developed smartphone based PDR can detect the motion of pedestrian step accurately. In the other words, it is capable of distinguishing the pedestrian motion in walking or standing. In the standing mode, the Kalman filter should rely on the PDR much more than 3D-GNSS because of the strong GNSS NLOS effects mentioned earlier. Thus, small K^{PDR} and K^{ϑ} are applied and they are 0.01, and $(1^o)^2$, respectively. In the walking mode, the K^{PDR} and K^{ϑ} are set empirically as 2 and $(15^o)^2$, respectively.

IV. Experiments and Discussion

A. Experiment Setup

The experiments are conducted in Shinjuku area of Tokyo city as shown in Figs 1 and 2. The smartphone and commercial GNSS used are Nexus 5 and u-blox M8, respectively. Their attachments are shown in Fig. 7. We use u-blox M8 instead of Nexus to provide GNSS measurement because 3D-GNSS requires raw GNSS measurement (pseudorange). Currently, the Android API does not provide pseudorange measurement. If the smartphone could provide it, then the commercial GNSS receiver will be no longer need in the proposed system.

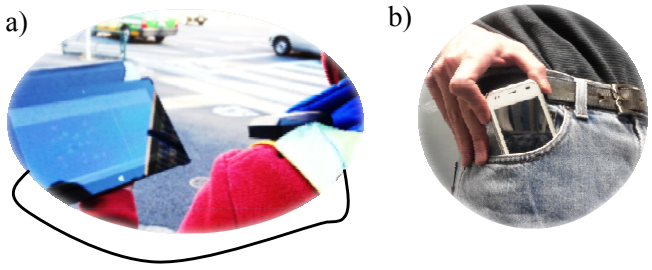

Fig. 7. Attachments of (a) u-blox path antenna and (b) Nexus smartphone.

B. 3D-GNSS in Urban Canyon with/without foliage

Both the data that not-affected and affected by foliage in this evaluation are the same with the data shown in Figs. 3 and 4. The positioning results are shown in Fig. 8. The performance evaluation is shown in TABLE I. This paper evaluates the lateral positioning error. Availability means the percentage of

solutions in a fix period. For example, if a method outputs 80 epochs in a 100 second period, the availability of the method is 80%. As can be seen from the right of Fig. 8, the 3D-GNSS can estimate accurate solutions. The mean and standard deviation of positioning error are about 1.5 and 1.4 meters, respectively. Comparing to the right of Fig. 8, both 3D-GNSS and u-blox cannot achieve satisfactory performance using the data attenuated by dense foliage. 3D-GNSS only gives about one-third of the solutions. In some points, 3D-GNSS gives the solution at the wrong side of street, which labelled in blue and green. Significantly, the calculated noise variance of the 3D-GNSS successfully represent the reliability of its solution. With regards to the commercial receiver, it is difficult to estimate the quality of their solutions. In general, the commercial GNSS receivers implement strong filtering technique to guarantee the smooth navigation service. This filtering technique also limits its use in the sensor integration system. We will demonstrate this limitation in the following subsections.

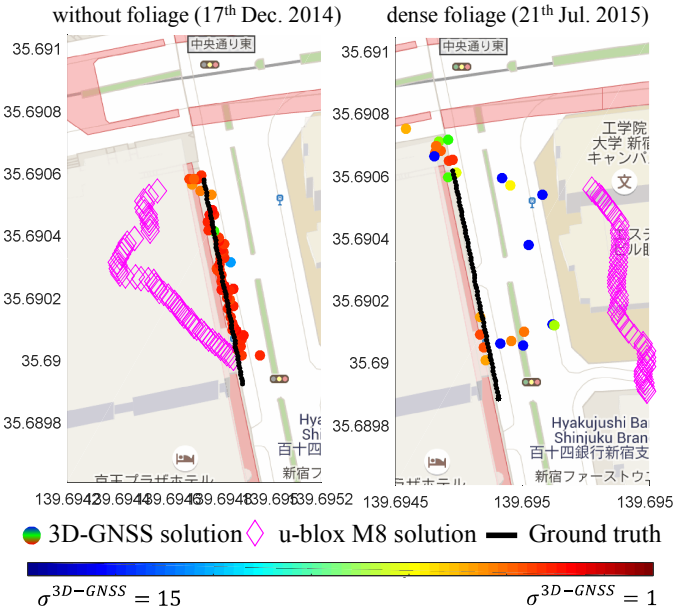

Fig. 8. Positioning results of 3D-GNSS (color dots) and u-blox M8 (pink dimands) in the deep urban canyon with/without dense foliage. Color of dots denotes the noise variance of the positioning performance of the 3D-GNSS.

TABLE I. POSITIIOING PERFORMANCE OF 3D-GNSS AND U-BLOX M8 IN THE DEEP URBAN CANYON WITH/WITHOUT DENSE FOLIAGE.

Deep urban canyon without foliage (17th Dec. 2014)			
Methods	Mean	Std.	Avail.
u-blox M8	20.2 m	9.6 m	100%
3D-GNSS	1.5 m	1.4 m	95.2%
Deep urban canyon with foliage (21th Jul. 2015)			
Methods	Mean	Std.	Avail.
u-blox M8	52.3 m	5.7 m	100%
3D-GNSS	9.6 m	9.1 m	33.3%

C. *Smartphone PDR*

The smartphone PDR used in this paper is a pocket-based PDR. The measurement of MEMS gyroscope becomes very noisy in the setup. Thus, this PDR uses only the accelerometer and magnetometer to estimate the heading direction of pedestrians. However, the magnetometer could be easily affect by the nearby ferrous objects, which resulted in a large bias in the heading estimation as demonstrated in Fig. 9. The tests included two turning motions and stopped in two intersections. In general, the rate of step detection is high (above 95%). As can be seen from Fig. 9, the shape and size of walking trajectory are very similar to the ground truth. Unfortunately, the error of heading direction is roughly between 10 to 45 degrees. Even through, the PDR only is not satisfactory, it is still able to provide the dynamic model of pedestrians.

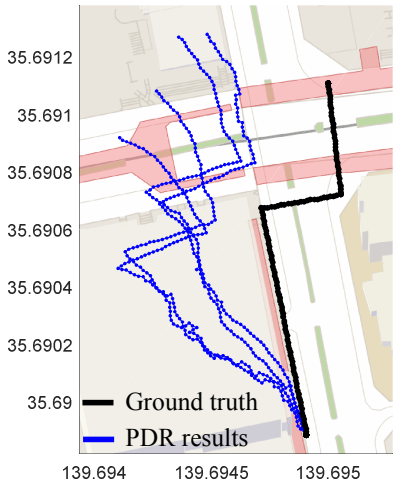

Fig. 9. Deomstration of the estimated pedestrian trajectories by the pocket-based smartphone PDR.

D. *Proposed Sensor Integration*

The data shown in the right of Fig. 8 is also used in this subsection. We do not evaluate the whole trajectory shown in Fig. 9 because the latter parts (two intersections) are not covered by street trees. The result of the proposed integration system is shown in Fig. 10. The smartphone PDR, again, could roughly depict the pedestrian heading direction. First, the improvement of the commercial receiver integrating with the PDR is insignificant. This is because the measurement noise covariance (R) of the receiver solution is set as constant. We have tried different values of R to find the best performance. However, in this kind of environment, an adaptive tuning is essential. As shown in TABLE II, The result of 3D-GNSS integrates with the PDR achieves approximately 4.4 and 2.5 meters in terms of mean and standard deviation of positioning error, respectively. Comparing TABLEs I and II, the availability increases from 33.3% to 100%. As can be seen from Fig. 10, the red dots denote the epochs that 3D-GNSS has solutions. According to Fig. 8, the noise variance of 3D-GNSS can depict the reliability of the solutions. Therefore, the 3D-GNSS solutions at correct side of street are given low $\sigma^{3D-GNSS}$ values, which equals to given high weighting to 3D-GNSS in the Kalman filtering integration. As a result, the integrated result is not biased to incorrect position.

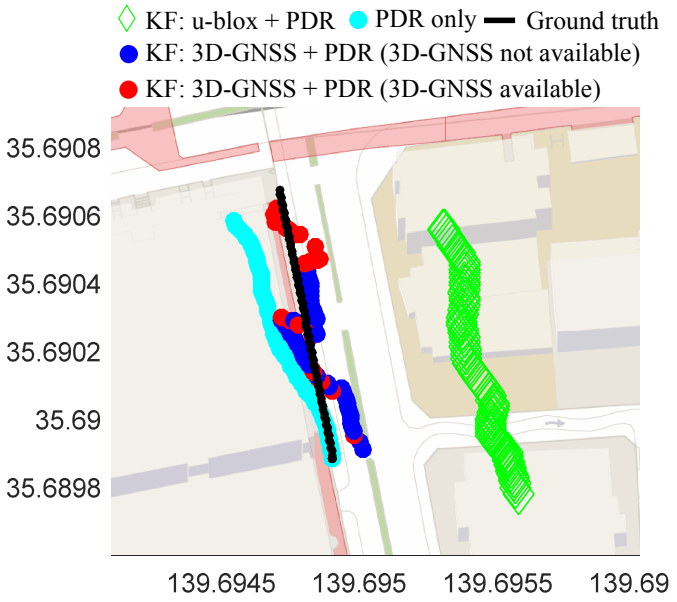

Fig. 10. Positioning integrated results of 3D-GNSS (blue and red dots) and u-blox M8 (green dimands) with the smartphone PDR (cyan dots) in the deep urban canyon with dense foliage.

TABLE II. POSITIIOING PERFORMANCE OF OF 3D-GNSS AND U-BLOX M8 WITH THE SMARTPHONE PDR IN THE DEEP URBAN CANYON WITH DENSE FOLIAGE

Integration with smartphone PDR (21th Jul. 2015)			
Methods	Mean	Std.	Avail.
PDR + u-blox M8	52.7 m	5.3 m	100%
PDR + 3D-GNSS	4.4 m	2.5 m	100%

V. CONCLUSIONS AND FUTURE WORK

In deep urban canyons, only a few number of the LOS visible satellites can be received. Due to the attenuation of dense foliage, the number of the trackable LOS satellites became even less. Comparing to LOS signals, NLOS GNSS signals are less influenced by foliage. Thus, it is important to use instead of excluding the NLOS reception. With the use of 3D-GNSS, the NLOS delay could be corrected using 3D building model and ray-tracing techniques. However, when the number of received satellite is less than the minimum requirements (4 and 5 for GPS and GNSS cases, respectively), inertial sensors are required. This paper successfully demonstrates that the performance of a loosely-coupled Kalman filter based integration between 3D-GNSS and smartphone PDR can achieve about 4.5 meters in lateral error with 100% availability.

This paper proves 3D-GNSS/PDR integration is useful even if the number of received satellite is few. However, in indoor areas (i.e., shopping mall, tunnel and under bridge), GNSS signals become very difficult (almost impossible) to be received. For vision impaired pedestrians, seamless localization service is required. The smartphone PDR is still capable of providing the dynamic model. To provide a global position information, Wi-Fi positioning could be a very good candidate. In addition, the smart-glasses (such as Google glasses) equipped with stereo camera is able to detect the obstacles and even to do visual odometry. Our future work is to integrate these sensors to provide localization service in the area that GNSS signal not available.

ACKNOWLEDGMENT

The authors acknowledge the Grant-in-Aid for Japan Society for the Promotion of Science (JSPS) Postdoctoral Fellowship for Oversea Researchers.

REFERENCES

[1] P. D. Groves, *Principles of GNSS, Inertial, and Multi-Sensor Integrated Navigation Systems (GNSS Technology and Applications)*, 2nd ed.: Artech House Publishers, 2013.

[2] M. G. Petovello and P. D. Groves. (2013) Multipath vs. NLOS signals. *Inside GNSS*. 40-42.

[3] L.-T. Hsu, S.-S. Jan, P. Groves, and N. Kubo, "Multipath mitigation and NLOS detection using vector tracking in urban environments," *GPS Solutions,* vol. 19, pp. 49-262, April 2015.

[4] P. D. Groves and Z. Jiang, "Height Aiding, C/N 0 Weighting and Consistency Checking for GNSS NLOS and Multipath Mitigation in Urban Areas," *The Journal of Navigation,* vol. 66, pp. 653-669, 2013.

[5] H. Tokura, H. Yamada, N. Kubo, and S. Pullen, "Using Multiple GNSS Constellations with Strict Quality Constraints for More Accurate Positioning in Urban Environments," *Positioning,* vol. 5, pp. 85-96, 2014.

[6] T. Suzuki and N. Kubo, "GNSS Positioning with Multipath Simulation using 3D Surface Model in Urban Canyon," in *ION GNSS 2012*, Nashville, TN, 2012, pp. 438 - 447.

[7] P. D. Groves, "Shadow Matching: A New GNSS Positioning Technique for Urban Canyons," *The Journal of Navigation,* vol. 64, pp. 417-430, 2011.

[8] A. Bourdeau, M. Sahmoudi, and J. Y. Tourneret, "Constructive use of GNSS NLOS-multipath: Augmenting the navigation Kalman filter with a 3D model of the environment," in *Information Fusion (FUSION), 2012 15th International Conference on*, 2012, pp. 2271-2276.

[9] G. Fu, L. Pu, and J.-C. Liu, "Line-Of-Sight Based Multipath Avoidance for GNSS Signals: Data Structures and Algorithms," in *Proceedings of ON GNSS+ 2015*, Tampa, Florida, 2015, pp. 2067-2078.

[10] P. D. Groves, L. Wang, M. Adjrad, and C. Ellul, "GNSS Shadow Matching: The Challenges Ahead," in *Proceedings of ION GNSS+ 2015*, Tampa, Florida, 2015, pp. 2421-2443.

[11] S. Miura, L. T. Hsu, F. Chen, and S. Kamijo, "GPS Error Correction With Pseudorange Evaluation Using Three-Dimensional Maps," *Intelligent Transportation Systems, IEEE Transactions on,* pp. 1-12, 2015. to be published. doi: 10.1109/TITS.2015.2432122.

[12] L.-T. Hsu, Y. Gu, F. Chen, Y. Wada, and S. Kamijo, "Assessment of QZSS L1-SAIF for 3D Map-Based

Pedestrian Positioning Method in an Urban Environment," in *Proceedings of ION ITM*, Dana Point, California, 2015.

[13] L.-T. Hsu, Y. Gu, and S. Kamijo, "3D building model-based pedestrian positioning method using GPS/GLONASS/QZSS and its reliability calculation," *GPS Solutions,* pp. 1-16, 2015. to be published. doi:10.1007/s10291-015-0451-7

[14] L.-T. Hsu, Y. Gu, and S. Kamijo, "NLOS Correction/Exclusion for GNSS Measurement Using RAIM and City Building Models," *Sensors,* vol. 15, pp. 17329-17349, 2015.

[15] N. Kakiuchi and S. Kamijo, "Pedestrian dead reckoning for mobile phones through walking and running mode recognition," in *Intelligent Transportation Systems - (ITSC), 2013 16th International IEEE Conference on*, 2013, pp. 261-267.